Extractive Bioconversion in a Four-Phase External-Loop Airlift Bioreactor

Lidija Sajc
Dept. of Analytical Chemistry, Faculty of Technology, Belgrade University, Belgrade, Yugoslavia

Gordana Vunjak-Novakovic
Division of Health Sciences and Technology, Massachusetts Institute of Technology, Cambridge, MA 01239

The integration of biosynthesis and product separation can increase the productivity of immobilized plant cells in airlift bioreactors. Extractive bioconversion of anthraquinones was studied in an external-loop airlift bioreactor consisting of a riser, a downcomer, and two horizontal sections, while containing alginate-immobilized Frangula alnus cells, a continuous aqueous phase (nutrient solution), dispersed solvent phase (n-hexadecane or silicone oil), and gas bubbles. A simple mathematical model was developed to describe the cocurrent liquid-liquid extraction in the riser section of the bioreactor and to rationalize the measured product concentrations in the aqueous and solvent phase. The model equations were solved analytically in a dimensionless form and used to study the effects of flow conditions, solvent properties, product formation rate, droplet size, and contactor length on the extraction efficiency and product concentration profiles in the continuous and dispersed phase.

Introduction

The incorporation of an extractive step can improve the productivity of immobilized cells and enzymes, increase product concentration in the outlet stream, and reduce the downstream volumes (Roffler et al., 1984; Mattiasson and Larsson, 1985; Daugulis et al., 1987; Mavituna et al., 1988; Daugulis, 1981; Collins and Daugulis, 1997). Various configurations of membrane bioreactors, which can contain high concentrations of immobilized cells but often involve diffusional limitations of mass transport, have been considered for use in extractive bioconversions (Cho and Shuler, 1986; Dahuron and Cussler, 1988; Belfort, 1989). Airlift bioreactors are an attractive alternative to membrane bioreactors, because they can provide high rates of mass transfer and efficient mixing in an environment permissive for cultivation of shear sensitive plant and mammalian cells (Buitelaar and Tramper, 1992).

For a given application, airlift bioreactors can be optimized with respect to: (a) cell support to achieve spatially uniform cell distribution; (b) mass-transfer rates to maintain the concentrations of nutrients and metabolites at desired levels; (c) bioreactor fluid dynamics to allow or even stimulate the expression of differentiated cell phenotype (Verlaan et al., 1986, 1989; Merchuk, 1991; Strobel et al., 1991; Taticek et al., 1994). Flow and mixing are known to affect the cultured cells in at least two ways: by flow-induced changes in mass transfer of chemical species, and by direct hydrodynamic effects on cell shape and function. Ideally, bioreactors should provide efficient mixing and mass transfer without adversely affecting cell growth and function (Holden and Yeoman, 1987; Brodelius and Pedersen, 1993; Vunjak-Novakovic et al., 1996; Sajc et al., 1999).

One important aspect of bioreactor design is the control the rate-limiting steps in biosynthetic pathways by *in situ* product removal in order to: (a) shift the equilibrium towards product formation; (b) remove products from an environment which can cause their degradation; (c) increase biosynthetic rates by reducing feedback inhibition of biosynthesis. Extractive bioconversion can be carried out in two ways: a liquid or solid extraction phase can be added directly to the bioreactor; or culture medium can be cycled to an external vessel containing an extraction medium. Adding the solvent directly to the bioreactor is simpler, but can lead to the formation of

Correspondence concerning this article should be addressed to G. Vunjak-Novakovic.

stable emulsion of organic phase in aqueous medium due to high shear rates required for the solvent dispersion. The formation of very small solvent drops can be eliminated by using columns where shear is lower and more uniform. In both cases, however, process design is complicated by product formation during extraction.

Previous studies of extractive bioconversions focused on low-molecular weight alcohols and organic acids (Roffler et al., 1987a,b) and in only a few cases on more complex products, such as volatile essential oils and alkaloids (Becker et al., 1984; Parr et al., 1987; Gontier et al., 1994). Mathematical models have been proposed for only a limited number of situations of interest for the present work, including, in particular, ethanol production by extractive fermentation in a continuous-stirred tank (Kollerup and Daugulis, 1985), extractive fermentation in an extermal-loop extraction column with countercurrent flow (Roffler et al., 1988), and cocurrent mass transfer with backmixing (Hartland and Mecklenburgh, 1969).

In the present work, we chose the production of anthraquinones by immobilized plant cells (Frangula alnus in alginate particles) as a model system for airlift bioreactors integrating the biosynthesis and separation within a single unit. The external loop airlift bioreactor studied was a four-phase system, with a continuous aqueous phase containing nutrients, immobilized cells, and dispersed gas and solvent phase (Sajc et al., 1995a). We proposed a simple mathematical model of cocurrent liquid-liquid extraction in the riser flow, in the form of two second-order differential equations, which were solved analytically in nondimensionless form and used to analyze the effects of flow and mass transfer on product extraction.

Experimental Setup

Batch cultivation of immobilized cells was performed in a 250 mL volume external loop bioreactor shown in Figure 1. The vessel was composed of a riser (2.7-cm ID), a downcomer (1.7-cm ID), and two horizontal sections. A gas-liquid-liquid separator on the top of the vessel provided complete degassing of the aqueous phase, and coalescence of the dispersed solvent droplets. A sintered glass plate (160 μm pore size) was used for air distribution with five symmetrically positioned 1-mm diameter holes for solvent distribution. Frangula alnus cells were derived from seedlings and maintained *in vitro* in callus and suspension cultures as previously described (Sajc et al., 1995b). Suspended cells cultured for four weeks in shake flasks were immobilized in 2.5-mm diameter alginate particles (Sajc et al., 1995b). In the circulating regime, a four-phase (gas-liquid-liquid-solid) and a two-phase (liquid-solid) flow were established in the riser and downcomer sections of the bioreactor, respectively. The density, viscosity, and surface tension of silicone oil and *n*-hexadecane, which were used as solvents, were 960 and 773 kg/m^3, 0.05 and 0.003 Pa·s, and 22 and 28 mN/m, respectively. The superficial velocities of gas (0.2–1.2 cm/s) and solvent (0.01–0.2 cm/s), the volume fraction of alginate particles (0–50%), volumetric holdup of gas and solvent, liquid circulation velocity, mixing in the aqueous phase, and mass-transfer coefficients of oxygen and plant cell products were determined as previously described (Sajc et al., 1995a). In order to provide complete coalescence of the solvent droplets, the superficial velocities of solvent and gas phase were set to 0.04 and 0.4 cm/s, respectively, and the volumetric fraction of calcium alginate particles was set to 30%. Under these conditions, both the gas and solvent holdup were approximately 1.2%, the superficial velocity of aqueous phase was 4 cm/s, axial dispersion coefficient was 19.7 cm^2/s, and the diameters of silicone oil and *n*-hexadecane droplets were 8 and 5 mm, respectively (Sajc et al., 1995b).

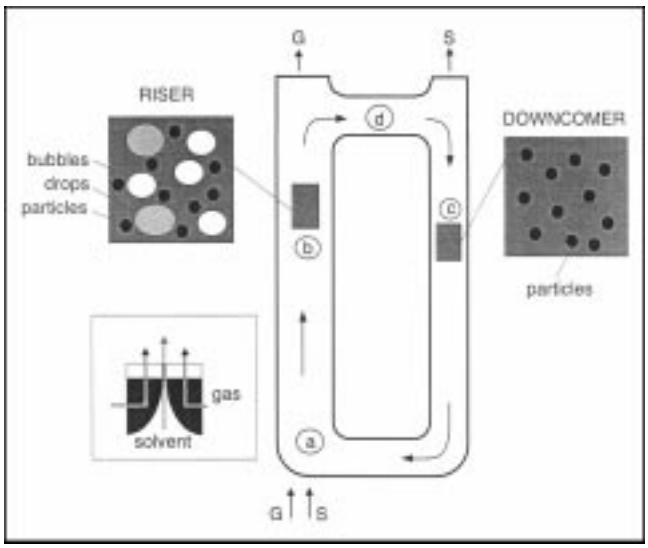

Figure 1. Experimental setup.

Extractive bioconversion of anthraquinons by plant cells (Fragnula alnus) immobilized in alginate particles was studied in a 250 mL volume external-loop airlift bioreactor consisting of (a) inlet region (distribution of gas and solvent), (b) riser (aqueous phase with alginate particles, gas bubbles and solvent drops), (c) downcomer (aqueous phase with alginate particles), and (d) upper section (separation of gas and solvent). The bioreactor was operated at steady-state conditions with a continuous flow of gas and solvent.

Modeling

For an irreversible, zero-order reaction with no accompanying volume change, a mass balance of product in the continuous phase of a differential section with one-dimensional cocurrent flow of a continuous and a dispersed liquid phase (Figure 2) involves five terms as follows

$$\frac{\partial c_x}{\partial t} - D_x \frac{\partial^2 c_x}{\partial z^2} + u_x \frac{\partial c_x}{\partial z} + k_l a(c_x - c_x^*) + \tau_x = 0 \qquad (1)$$

The corresponding equation for the dispersed liquid phase is

$$\frac{\partial c_y}{\partial t} - D_y \frac{\partial^2 c_y}{\partial z^2} + u_y \frac{\partial c_y}{\partial z} + k_l a(c_x - c_x^*) + \tau_y = 0 \qquad (2)$$

where c_x and c_y (g/L) are product concentrations, D_x and D_y (cm^2/s) are axial dispersion coefficients, u_x and u_y (cm/s) are superficial velocities, τ_x and τ_y [g/(L·s)] are reaction rate constants in the continuous and dispersed liquid phase, re-

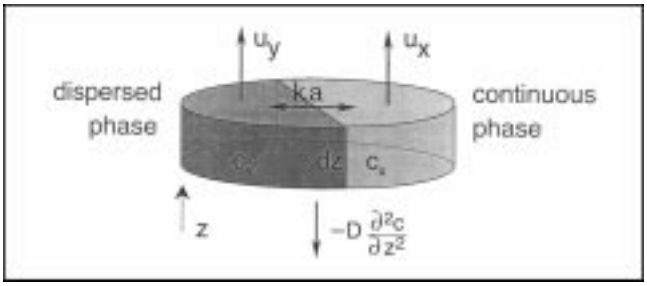

Figure 2. One-dimensional two-phase model.

Cocurrent flow of the continuous (aqueous) and dispersed (solvent) phase in the riser section of the bioreactor, where c_x and c_y (g/L) are product concentrations, u_x and u_y (cm/s) are superficial velocities for the continuous and dispersed phase, respectively, and z is the vertical position within the section.

spectively, and $k_l a$ (1/s) is the overall mass-transfer coefficient for the product, based on the continuous phase.

Equations 1 and 2 may be simplified by assuming: (1) steady-state operation (transient term can be eliminated); (2) no reaction in the dispersed solvent phase (τ_y term can be eliminated from Eq. 2). The resulting relationships are second-order differential equations which can be solved analytically

$$\frac{\partial^2 c_x}{\partial z^2} - \frac{u_x}{D_x}\frac{\partial c_x}{\partial z} - \frac{k_l a}{D_x}(c_x - c_x^*) + \frac{\tau_x}{D_x} = 0 \qquad (3)$$

$$\frac{\partial^2 c_y}{\partial z^2} - \frac{u_y}{D_y}\frac{\partial c_y}{\partial z} - \frac{k_l a}{D_y}(c_x - c_x^*) = 0 \qquad (4)$$

Assuming a linear equilibrium relationship

$$c_x^* = mc_y \qquad (5)$$

where m (1) is the slope of equilibrium line dc_x/dc_y, Eqs. 3 and 4 can be expressed as

$$\frac{d^2 c_x}{dz^2} - \frac{u_x}{D_x}\frac{dc_x}{dz} - \frac{k_l a}{D_x}(c_x - mc_y) + \frac{\tau_x}{D_x} = 0 \qquad (6)$$

$$\frac{d^2 c_y}{dz^2} - \frac{u_y}{D_y}\frac{dc_y}{dz} - \frac{k_l a}{D_y}(c_x - mc_y) = 0 \qquad (7)$$

or, using simpler notation

$$X'' - AX' - BX + CY + D = 0 \qquad (8)$$

$$Y'' - EY' + FX - GY = 0 \qquad (9)$$

where $A = u_x/D_x$, $B = k_l a/D_x$, $C = (k_l a \cdot m)/D_x$, $D = \tau_x/D_x$, $E = u_y/D_y$, $F = k_l a/D_y$ and $G = (k_l a \cdot m)/D_y$. The homogeneous solutions to Eqs. 3 and 4 are in the form $X_h = a \cdot e^{\lambda z}$ and $Y_h = b \cdot e^{\lambda z}$. Inserting X_h and Y_h in Eqs. 8 and 9 yields the characteristic equation

$$\lambda^4 - \lambda^3(A + E) - \lambda^2(G - AE + B) + \lambda(AG + BE) - (CF - BG) = 0 \qquad (10)$$

which, for $BG = CF$, reduces to

$$\lambda^3 - \lambda^2(A + E) - \lambda(G - AE + B) + (AG + BE) = 0 \qquad (11)$$

and $\lambda_1 = 0$.

The general solutions of Eqs. 3 and 4 are

$$X = a_1 + a_2 \cdot e^{\lambda_2 \cdot z} + a_3 e^{\lambda_3 \cdot z} + a_4 e^{\lambda_4 \cdot z} + X_p \qquad (12)$$

$$Y = a_1\eta_1 + a_2\eta_2 \cdot e^{\lambda_2 \cdot z} + a_3\eta_3 e^{\lambda_3 \cdot z} + a_4\eta_4 e^{\lambda_4 \cdot z} + Y_p \qquad (13)$$

where

$$\eta_i = \frac{\lambda_i^2 - A\lambda_i - B}{-C} \qquad (14)$$

and X_p and Y_p are particulate solutions. If $\lambda_1 = 0$, then $\eta_1 = B/C$.

The solutions were assumed to be in the form

$$X_p = P_1 \cdot z + Q_1; \qquad Y_p = P_2 \cdot z + Q_2 \qquad (15)$$

and calculated as

$$X_p = \frac{DG^2}{AG^2 + CEF} z = P_1 z \qquad (16)$$

$$Y_p = \frac{F}{G}P_1 z - \frac{EF}{G^2}P_1 = P_2 z + Q \qquad (17)$$

For each set of parameters $A - G$, the roots of characteristic Eq. 11 λ_2, λ_3, and λ_4 were determined graphically to satisfy the condition given by Eq. 14.

The coefficients a_1, a_2, a_3, and a_4 in Eqs. 12 and 13 were obtained using the following boundary conditions

$$\left(\frac{dX}{dz}\right)_{z=L} = 0 \qquad (18)$$

$$\left(\frac{dY}{dz}\right)_{z=L} = 0 \qquad (19)$$

$$-\left(\frac{dX}{dz}\right)_{z=0} = A(X_F - X) \qquad (20)$$

$$\left(\frac{dY}{dz}\right)_{z=0} = E(Y - Y_F) \qquad (21)$$

where L (cm) is the length of the riser section, and X_F and Y_F (g/L) are product concentrations in the continuous and dispersed liquid phase, respectively, at the section inlet.

Substitution of λ_i, η_i, P_1, P_2, Q, L, and $A-G$ values in Eqs. 18–21 leads to four simultaneous algebraic equations

$$\sum_{i=1}^{4} a_i \lambda_i e^{\lambda_i L} = -P_1 \qquad (22)$$

$$\sum_{i=1}^{4} a_i \eta_i \lambda_i e^{\lambda_i L} = -P_2 \qquad (23)$$

$$\sum_{i=1}^{4} a_i(A-\lambda_i) = AX_F + P_1 \tag{24}$$

$$\sum_{i=1}^{4} a_i\eta_i(\lambda_i - E) = E(Q - Y_F) - P_2 \tag{25}$$

which were solved using matrix calculus to determine the concentration profiles along the chosen contactor length given by Eqs. 12 and 13.

Anomalous roots of Eq. 11 were also derived. One of the λ_i roots vanishes when

$$Pe_y \gg Pe_x \{\text{that is, } E \gg A\}, \text{ and}$$

$$Pe_x \gg Pe_y \{\text{that is, } A \gg E\}, \text{ and}$$

$$f = m \cdot u_x/u_y = 1 \{\text{that is, } AG + BE = 0, \text{ and } \lambda^2 - \lambda_i(A+E) - (G - AE + B) = 0\}$$

The above approach was used in the present work to determine the effects of product formation rate, axial dispersion in the continuous and dispersed liquid phase, solvent properties, and contactor length on cocurrent liquid-liquid extraction in the riser of an external loop airlift bioreactor with immobilized plant cells.

Results and Discussion

The product concentration profiles in the continuous X and dispersed liquid-phase Y in the riser section of the bioreactor shown in Figure 3 are model predictions for one representative series of experiments involving liquid-liquid extraction by *n*-hexadecane. The superficial gas and solvent velocities were set to 0.4 cm/s and 0.04 cm/s, respectively. A steady-state circulation of liquid and particles within the loop was maintained in the bioreactor without recirculation of gas bubbles and solvent drops into the downcomer region. At these conditions, the continuous liquid-phase velocity was $u_x = 4$ cm/s, the axial dispersion coefficient was $D_x = 19.7$ cm^2/s, and the slope of the equilibrium line was $m = dc_x/dc_y = 1/16.7$ (Sajc et al., 1995a). Under these conditions, the measured kinetic rate of product formation by immobilized cells in the bioreactor was constant and equaled $\tau_x = 1.45 \times 10^{-5}$ g/L·s (Sajc et al., 1995b). The axial dispersion coefficient in the dispersed phase was calculated according to Liou et al. (1991)

$$0.048\ Re_x^{0.294} Re_y^{1.299} = \frac{\epsilon_y D_y}{u_y d_d} \tag{26}$$

where $Re_x = u_x \rho_x d_d/\mu_x$ and $Re_y = u_y \rho_y d_d/\mu_y$ are Reynolds numbers for the continuous and dispersed phase, respectively.

Both the *n*-hexadecane and silicone drops were of intermediate size ($d_d = 5$–8 mm), and were characterized as ellipsoidal and oscillatory according to the values of Eotvos, Morton and Reynolds criteria ($Eo \sim 1-2$, log $M \sim -10$, $Re_T \sim 600$). Such droplets generally show two types of superimposed secondary motion: ''rocking'' along a zig-zag or spiral trajectory; and shape dilatations, usually referred to as ''oscillations.'' Oscillations can play an important role in increasing drag, reducing terminal velocities, and promoting mixing, heat and mass transfer at the droplet interfaces (Clift et al., 1978). Oscillations of *n*-hexadecane and silicone droplets were rapid ($Sc \gg 1$) and the internal mass-transfer resistance was thus assumed to be constant and independent of molecular diffusivity. The effects of oscillations on external mass-transfer resistance were considered to be significant, according to (Cliff et al., 1978, p. 191)

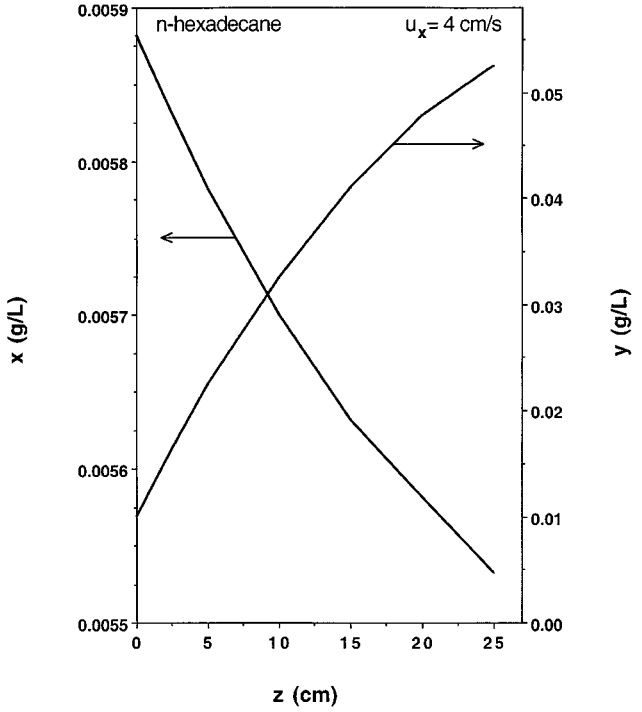

Figure 3. Product concentration profiles.

Profiles are in the continuous (x) and dispersed phase (y) for bioconversion involving product extraction with *n*-hexadecane at the superficial velocities of aqueous and solvent phase of $u_x = 4$ cm/s and $u_y = 0.4$ (cm/s), respectively, diameter of solvent droplets $d_d = 5$ (mm), and product formation rate $\tau_x = 1.45 \cdot 10^{-5}$(g/L·s).

$$\frac{d_d f_N}{u_T} > 0.15 \tag{27}$$

where d_d (m) is the average drop diameter, f_N (1/s) is Lamb's natural frequency of drop oscillations (Clift et al., 1978, p. 187)

$$f_N^2 = \frac{48\sigma}{\pi^2 d_d^3 \rho(2+3\gamma)} \tag{28}$$

u_T (m/s) is drop terminal velocity, σ (N/m) is the solvent-aqueous phase interface tension, and $\gamma = \rho_p/\rho$ is the ratio of liquid densities for the dispersed and continuous liquid phase.

The overall mass-transfer coefficient was calculated using an empirical equation for mass transfer controlled by a thin aqueous film around a droplet, in order to avoid uncertainties associated with the predictions of the frequency and am-

plitude of oscillations (Clift et al., 1978, p. 197)

$$k_l a = 7.2\sqrt{\frac{Df_N}{d_d^2}} \tag{29}$$

where $k_l a$ (1/s) is the overall mass-transfer coefficient and $D = 5.77\times10^{-10}$ (m^2/s) solute diffusivity in the continuous liquid phase, calculated using the Wilke and Chang (1955) correlation. The agreement of calculated and measured values for 3.5- and 5-mm *n*-hexadecane and 8-mm silicone oil drops in a four-phase flow was satisfactory (the average deviation was $<6\%$). The product concentration gradients within the aqueous liquid phase were found insignificant (Sajc et al., 1995a).

The characteristic Eq. 11 was solved graphically using $u_x = 4$ cm/s, $u_y = 0.04$ cm/s, $D_x = 19.7$ cm^2/s, $D_y = 0.16$ cm^2/s, $m = 1/16.7$, $\tau_x = 1.45\times10^{-5}$ g/(L·s), $k_l a = 0.023$ 1/s, and the values of coefficients $A-G$ ($A = 0.20$ 1/cm, $B = 1.17\times10^{-3}$ $1/cm^2$, $C = 7.0\times10^{-5}$ $1/cm^2$, $D = 7.36\times10^{-7}$ g/(L·cm^2), $E = 0.25$ 1/cm, $F = 0.144$ $1/cm^2$, $G = 8.61\times10^{-3}$ $1/cm^2$) to obtain $\lambda_1 = 0$, $\lambda_2 = 0.282$, $\lambda_3 = 0.206$, and $\lambda_4 = -0.0351$. The values of $\eta_1 = 16.7$, $\eta_2 = -3.01\times10^2$, $\eta_3 = -0.943$, and $\eta_4 = -1.01\times10^2$ were then calculated from Eq. 14. Equations 22–25 were solved by using the values of $P_1 = 3.1\times10^{-6}$ g/L·cm, $P_2 = 5.2\times10^{-5}$ g/L·cm, $Q = -1.51\times10^{-3}$ g/L, $L = 27$ cm, the inlet concentration of product in the solvent phase $y_F = 0$, and aqueous phase $x_F = 6.0\times10^{-3}$ g/L to obtain the coefficients $a_1 = 5.15\times10^{-3}$, $a_2 = 6.16\times10^{-9}$, $a_3 = 6.32\cdot10^{-8}$, and $a_4 = 7.35\times10^{-4}$, which were then used to solve Eqs. 12 and 13 and obtain concentration profiles shown in Figure 3. The product concentration in the continuous phase X decreased from 6 to 5.88 mg/L, presumably due to axial dispersion, while the product concentration in the dispersed liquid phase Y increased from 0 to 0.01 g/L. At the riser outlet, product concentrations in the aqueous and dispersed liquid phase were 5.55 mg/L and 0.05 g/L, respectively.

Figure 4 shows the corresponding model predictions for product extraction by silicone oil. Silicone drops were larger than *n*-hexadecane drops ($d_d = 8$ and 5 mm, respectively, at $u_x = 4$ cm/s and $u_y = 0.04$ cm/s), due to the lower viscosity and density and higher interphase tension of *n*-hexadecane. Consequently, the values of the axial dispersion coefficient in the dispersed liquid phase $D_y = 0.018$ cm^2/s, the slope of equilibrium line $m = 1/13.8$, and the mass-transfer coefficient $k_l a = 0.0125$ 1/s were all lower than the corresponding values for *n*-hexadecane. The characteristic Eq. 11 was solved graphically using the values $A = 0.20$ 1/cm, $B = 6.34\times10^{-4}$ $1/cm^2$, $C = 4.61\times10^{-5}$ $1/cm^2$, $D = 7.36\times10^{-7}$ g/L·cm^2, $E = 2.22$ 1/cm, $F = 0.694$ $1/cm^2$, $G = 0.05$ $1/cm^2$, $P_1 = 3.18\times10^{-6}$ g(L·cm, $P_2 = 4.41\times10^{-5}$ g/L·cm, $Q = -1.96\times10^{-3}$ g/L, $\lambda_1 = 0$, $\lambda_2 = 2.24$, $\lambda_3 = 0.189$, $\lambda_4 = -0.021$, $\eta_1 = 13.8$, $\eta_3 = 7.11$, $\eta_4 = -88.5$, $L = 27$ cm, $y_F = 0$, $x_F = 6.0\times10^{-3}$ g/L, $a_1 = 5.16\times10^{-3}$, $a_3 = 1.97\times10^{-7}$, and $a_4 = 7.75\times10^{-4}$. The second terms in Eqs. 12 and 13 were omitted, based on the value $a_2 = 2.2\times10^{-35}$. Concentration "jumps" in continuous and dispersed liquid phase at the contactor inlet, 6–5.9 mg/L and 0–0.18 mg/L, respectively, were lower than the corresponding values for *n*-hexadecane (Figure 3). For the same rate of product formation, ΔX and ΔY were 0.22 and 31.3 mg/L, respectively, and the efficiencies of extraction by silicone oil and *n*-hexadecane were comparable.

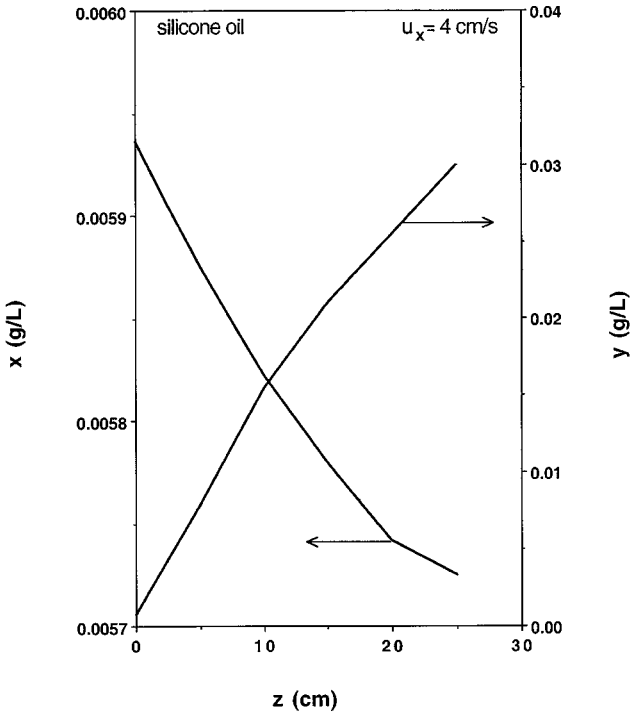

Figure 4. Product concentration profiles in the continuous (x) and dispersed phase (y).

Profiles are for bioconversion involving product extraction with silicone oil at the superficial velocities of aqueous and solvent phase of $u_x = 4$ cm/s and $u_y = 0.4$ (cm/s), respectively, diameter of solvent droplets $d_d = 8$ (mm), and product formation rate $\tau_x = 1.45\cdot10^{-5}$ (g/L·s).

Figure 5 shows the model prediction for the effect of the total length of the contactor L on product concentration in the continuous phase X; the operating conditions are the same as for Figure 3. The predicted behavior can be attributed to the counteracting effects of mass transfer (which decreases as the contactor length increases) and product formation (which is independent of contactor length). In general, X decreases with an increase in the contactor length, until the average rate of mass transfer in the contactor becomes equal to the average rate of product formation ($L = 60$ cm in Figure 5). At these conditions, the solute concentration passes through a minimum, and any further increase in the contactor length results in an increase in solute concentration in raffinate, due to the decrease in the driving force for mass transfer. The corresponding value of solute concentration in the dispersed phase Y increases continuously as the length of the contactor increases (Figure 6). However, the increase in Y is slower in the range $60 < L < 340$ cm, than for $15 < L < 60$ cm, which is consistent with the limitations identified by Pratt (1975) and Roffler et al. (1988) for countercurrent contact at $L > 1.3$ m.

The model predictions of the effects of product formation rate τ_x on product concentration in the continuous liquid phase X along the contactor length is shown in Figure 7 for liquid-liquid extraction by *n*-hexadecane; the operating conditions are the same as those in Figure 3. If the rate of prod-

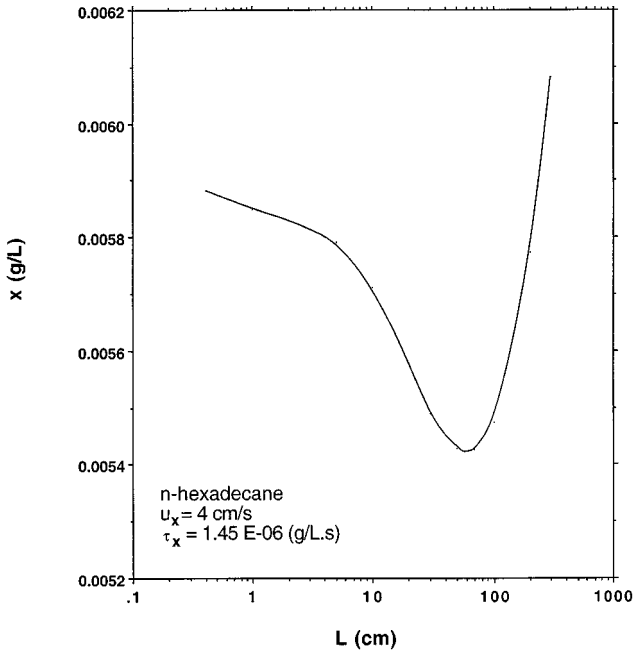

Figure 5. Effect of the length of contactor on the outlet product concentration in the continuous phase (x).

For bioconversion involving product extraction with *n*-hexadecane at the superficial velocities of aqueous and solvent phase of $u_x = 4$ cm/s and $u_y = 0.4$ (cm/s), respectively, diameter of solvent droplets $d_d = 5$ (mm), and product formation rate $\tau_x = -1.45 \cdot 10^{-5}$ (g/L·s).

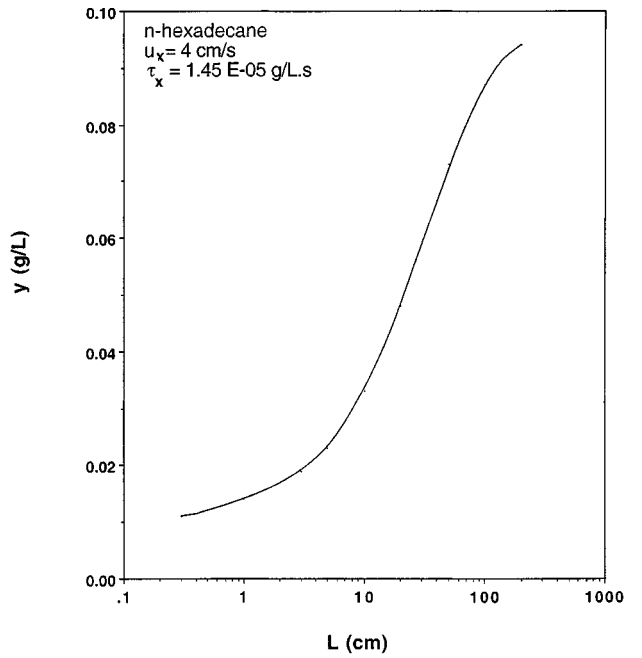

Figure 6. Effect of the length of contactor on the outlet product concentration in the dispersed phase (y).

Effect is for bioconversion involving product extraction with *n*-hexadecane, at the superficial velocities of aqueous and solvent phase of $u_x = 4$ cm/s and $u_y = 0.4$ (cm/s), respectively, diameter of solvent droplets $d_d = 5$ (mm), and product formation rate $\tau_x = 1.45 \cdot 10^{-5}$ (g/L·s).

uct formation exceeds the rate of mass transfer, the outlet concentration of the product becomes higher than the feed concentration. For example, for $\tau_x = 1.45 \cdot 10^{-4}$ g/L·s, the product concentration in the continuous phase "jumps" from 6 to 6.5 mg/L at the inlet, and equals 6.4 mg/L at the outlet.

Figure 8 shows the model predictions for product concentrations in the continuous X and dispersed phase Y for extraction by *n*-hexadecane at $u_x = 10$ cm/s, calculated using: $A = 0.15$ 1/cm, $B = 6.0 \times 10^{-4}$ 1/cm^2, $C = 3.6 \times 10^{-5}$ 1/cm^2, $D = 2.17 \times 10^{-7}$ g/L·cm^2, $E = 0.625$ 1/cm, $F = 0.625$ 1/cm^2, $G = 3.74 \times 10^{-2}$ 1/cm^2, $P_1 = 1.35 \times 10^{-6}$ g/L·cm, $P_2 = 2.27 \times 10^{-5}$ g/L·cm, $Q = -3.79 \times 10^{-4}$ g/L, $\lambda_1 = 0$, $\lambda_2 = 0.68$, $\lambda_3 = 0.15$, $\lambda_4 = -0.058$, $\eta_1 = 16.7$, $\eta_3 = -5.19$, $\eta_4 = -3.16 \times 10^{-2}$, $L = 27$ cm, $y_F = 0$, $x_F = 6.0 \times 10^{-3}$ g/L, $a_1 = 5.63 \times 10^{-3}$, $a_3 = 2.05 \times 10^{-7}$, and $a_4 = 2.71 \times 10^{-4}$. The second terms in Eqs. 12 and 13 were disregarded, based on $a_2 = 1.65 \times 10^{-16}$.

Comparison of product concentration profiles in Figure 3 ($u_x = 4$ cm/s) and Figure 8 ($u_x = 10$ cm/s) shows that u_x affects the contactor performance in three ways, as follows. First, the extent of backmixing in the continuous phase, which is proportional to the u_x/D_x ratio, will increase as u_x decreases. Second, the residence time of the continuous phase is inversely proportional to u_x, resulting in more product formation at lower superficial velocities. Third, the average diameter of liquid drops and gas bubbles will decrease as u_x increases. For example, *n*-hexadecane drops were 3.5 mm in diameter at $u_x = 10$ cm/s (Figure 8) as compared to 5 mm in diameter at $u_x = 4$ cm/s (Figure 3). The 3.5 mm diameter

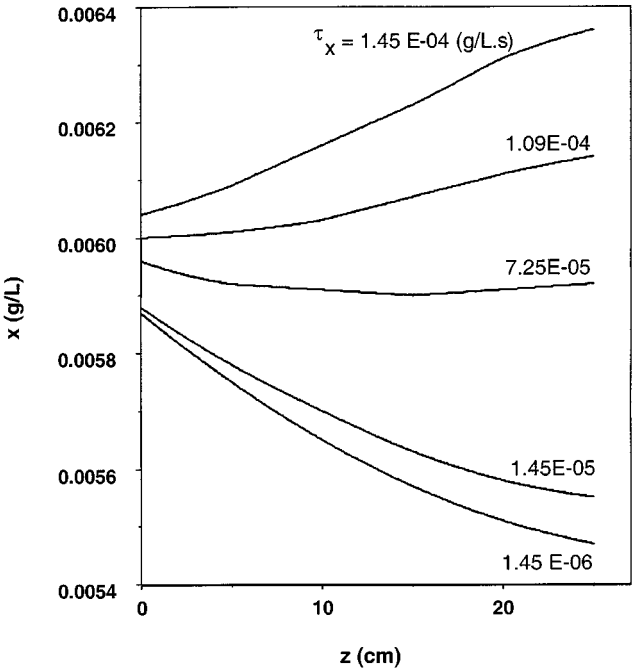

Figure 7. Concentration of cell product in the continuous phase (X) along the contactor as a function of product formation rate.

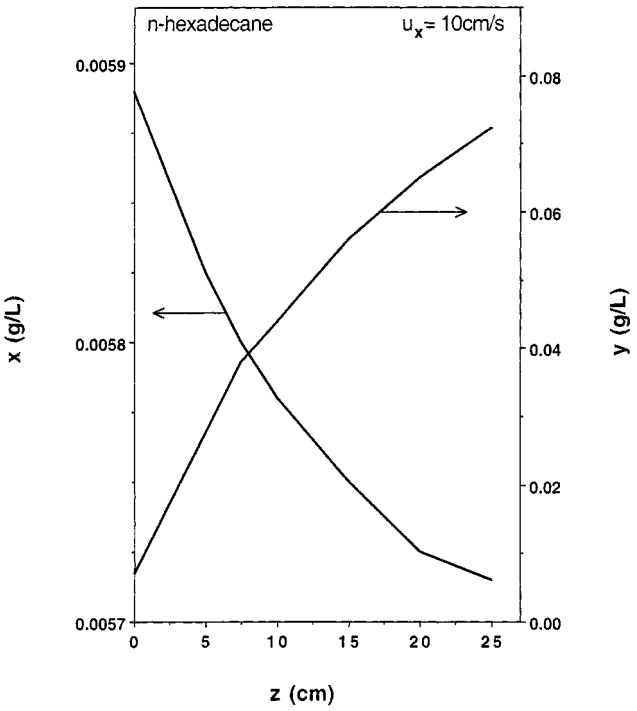

Figure 8. Effect of the superficial continuous phase velocity on the product concentration in continuous (X) and dispersed phase (Y).

drops were ellipsoidal and oscillatory, as were the 5 mm *n*-hexadecane and 8 mm silicone oil drops. The value of the axial dispersion coefficient for 3.5 mm *n*-hexadecane drops ($D_y = 0.064$ cm^2/s) was lower than that for 5 mm *n*-hexadecane drops (0.16 cm^2/s), but higher than for 8 mm silicone oil drops (0.018 cm^2/s) due to the low viscosity of silicone oil. For $u_x < 8$ cm/s (dispersed bubble regime), the u_x/D_x ratio was constant and equal to 0.20 1/cm ($u_x = 4$ cm/s, $D_x = 19.7$ cm^2/s), whereas for $u_x > 8$ cm/s (coalesced bubble regime), the ratio u_x/D_x was 0.15 1/s and $D_x = 66.7$ cm^2/s (Sajc et al., 1995a). At these conditions, the value of $k_l a = 0.04$ 1/s was significantly higher than for 5 mm *n*-hexadecane drops (0.023 1/s) and 8 mm silicone oil drops (0.0125 1/s). The amount of product stripped from continuous aqueous phase was 0.17 mg/L, as compared to 0.33 and 0.22 mg/L for 5 mm *n*-hexadecane and 8 mm silicone oil drops, respectively, due to more efficient mixing in the continuous liquid phase. The increase of product concentration in the dispersed phase was approximately 25% and 50% higher at these conditions than during extraction by *n*-hexadecane and silicone oil, respectively, at $u_x = 4$ cm/s, presumably due to the increased interfacial area available for mass transfer and improved mixing in the continuous liquid phase.

In summary, liquid-liquid extraction in a cocurrent four-phase flow in the riser of an external-loop airlift bioreactor with immobilized plant cells producing antraquinons was studied experimentally and described using a simple mathematical model. The proposed approach extends the work of Pratt (1975) and Roffler et al. (1988) on liquid-liquid extraction in countercurrent flow to the cocurrent flow in plant cell bioreactors. A set of two second-order differential equations was solved in a dimensionless form and used to study the effects of product formation rate, contactor length, mixing in the continuous phase, and droplet characteristics for the dispersed phase on the steady-state concentrations of the product in the aqueous (continuous) and solvent (dispersed) phase. The proposed model could be extended to the conditions of product formation in the dispersed phase, as well as other plant cell cultures and extracellular products.

Acknowledgments

This work was partially supported by Research Council of Serbia Grant No. 03-E-21 and the Serbian Academy of Sciences.

Literature Cited

Bakker, W. A. M., M. Denhertog, J. Tramper, and C. D. Degooijer, "Oxygen Transfer in a Multiple Airlift-Loop Reactor," *Bioprocess Eng.*, **12**, 167 (1995).

Becker, H., J. Reichling, W. Bisson, and S. Herold, "Two-Phase Culture—a New Method to Yield Lipophilic Secondary Products from Plant Suspension Cultures," *Third Eur. Congress on Biotechnol.*, Vol. 1, Dechema, Verlag-Chemie, Frankfurt, Germany, 209 (1984).

Belfort, G., "Membranes and Bioreactors: A Technical Challenge in Biotechnology," *Biotechnol. Bioeng.*, **33**, 1047 (1989).

Brodelius, P., and H. Pedersen, "Increasing Secondary Metabolite Production in Plant Cell Culture by Redirecting Transport," *Trends in Biotechnol.*, **11**, 45 (1993).

Buitelaar, M. R., and J. Tramper, "Strategies to Improve the Production of Secondary Metabolites with Plant Cell Culture: a Literature Review," *J. Biotechnol.*, **23**, 114 (1992).

Cho, T., and M. L. Shuler, "Multimembrane Bioreactor for Extractive Fermentation," *Biotechnol. Prog.*, **2**, 53 (1986).

Clift, R., J. R. Grace, and M. E. Weber, *Bubbles, Drops, and Particles*, Academic Press, New York (1978).

Collins, L. D., and A. J. Daugulis, "Characterization and Optimization of a Two-Phase Partitioning Bioreactor for the Biodegradation of Phenol," *Appl. Microbiol. Biotechnol.*, **48**, 18 (1997).

Cormier, F., and C. Ambib, "Extractive Bioconservation of Geraniol by a Vitis vinifera Cell Suspension Employing a Two-Phase System," *Plant Cell Rep.*, **6**, 427 (1987).

Dahuron, L., and E. L. Cussler, "Protein Extractions with Hollow Fibers," *AIChE J.*, **34**, 130 (1988).

Daugulis, A. J., D. E. Swaine, F. Kollerup, and C. A. Groom, "Extractive Fermentation—Integrated Reaction and Product Recovery," *Biotechnol. Lett.*, **9**, 425 (1987).

Daugulis, A. J., "Integrated Product Formation and Recovery," *Curr. Opin. Biotechnol.*, **2**, 408 (1991).

Forche, E., W. Schubert, W. Kohl, and G. Hofle, "Cell Culture of Thuja Occidentalis with Continuous Extraction of Excreted Terpenoids," *Eur. Cong. on Biotechnol.*, Vol. 1, Dechema, Frankfurt, Germany, Verlag-Chemie, 189 (1984).

Gontier, E., B. W. Sangwar, and J. N. Barbotin, "Effects of Calcium, Alginate, and Calcium-Alginate Immobilization on Growth and Tropane Alkaloid Levels of a Stable Suspension Cell Line of Datura Inoxia Mill," *Plant Cell Rep.*, **13**, 533 (1994).

Hartland, S., and J. C. Mecklenburgh, *The Analysis of Co-Current Mass Transfer Problems with Backmixing, in Co-Current Gas-Liquid Flow*, E. Rhodes and D. S. Scott, eds., Plenum Press, New York, p. 561 (1969).

Holden, A. M., and M. W. Yeoman, "Optimization of Product Yield in Immobilized Plant Cell Cultures," *Bioreactors and Biotransformation*, G. W. Moody and A. M. Holden, eds., Elsevier, London, p. 1 (1987).

Kollerup, F., and A. J. Daugulis, "A Mathematical Model for Ethanol Production by Extractive Fermentation in a Continuous Stirred Tank Fermentor," *Biotechnol. Bioeng.*, **27**, 1335 (1985).

Liou, T. C., S. S. Chang, and M. C. Wu, *J. Chin. Inst. Chem. Eng.*, **22**(3), 89 (1991).

Mattiasson, B., and M. Larsson, "Extractive Bioconversion with Emphasis on Solvent Production," *Biotechnol. Genet, Eng. Rev.*, **3**, 137 (1985).

Mavituna, F., A. K. Wilkinson, and P. D. Williams, "Liquid-Liquid

Extraction of Plant Secondary Metabolite as an Integrated Stage with Bioreactor Operation,'' *Separations for Biotechnology*, M. S. Verral and M. J. Hudson, eds., Ellis Horwood Ltd., Chichester, U.K., p. 333 (1988).
Merchuk, J. C., ''Shear Effects on Suspended Cells,'' *Advances in Biochemical Engineering and Biotechnology*, A. Fiechter, ed., Vol. 44, Springer-Verlag, Berlin, p. 65 (1991).
Parr, A. J., R. J. Robins, and M. J. C. Rhodes, ''Release of Secondary Metabolites by Plant Cell Cultures,'' *Plant and Animal Cells: Processes and Possibilities*, C. Webb and F. Mavituna, eds., Ellos Horwood, Chichester, U.K., p. 229 (1987).
Pratt, H. R. C., ''A Simplified Analytical Design Method for Differential Extractors with Backmixing: Linear Equilibrium Relationship,'' *Ind. Eng. Chem., Proc. Des. Dev.*, **14**, 74 (1975).
Roffler, S. R., H. W. Blanch, and C. R. Wilke, ''In Situ Recovery of Fermentation Products,'' *Trends Biotechnol.*, **2**, 129 (1984).
Roffler, S. R., H. W. Blanch, and C. R. Wilke, ''In situ Recovery of Butanol During Fermentation: I. Batch Extractive Fermentation, *Bioprocess. Eng.*, **2**, 1 (1987a).
Roffler, S. R., H. W. Blanch, and C. R. Wilke, ''In Situ Recovery of Butanol During Fermentation: II. Fed-Batch Extractive Fermentation,'' *Bioprocess. Eng.*, **2**, 83 (1987b).
Roffler, S. R., C. R. Wilke, and H. W. Blanch, ''Design and Mathematical Description of Differential Contactors Used in Extractive Fermentations,'' *Biotechnol. Bioeng.*, **32**, 192 (1988).
Sajc, L., B. Obradovic, D. Vukovic, B. Bugarski, D. Grubisic, and G. Vunjak-Novakovic, ''Hydrodynamics and Mass Transfer in a Four-Phase External-Loop Airlift Bioreactor,'' *Biotechnol. Prog.*, **11** 420 (1995a).
Sajc, L., G. Vunjak-Novakovic, D. Grubisic, N. Kovacevic, D. Vukovic, and B. Bugarski, ''Production of Anthraquinones by Immobilized Frangula alnus Mill. Plant Cells in a Four-Phase Airlift Bioreactor,'' *Appl. Microbiol. Biotechnol.*, **43**, 416 (1995b).
Sajc, L., N. Kovacevic, D. Grubisic, and G. Vunjak-Novakovic, ''In Vitro Culture of Frangula for the Production of Secondary Metabolites,'' *Biotechnology of Medicinal and Aromatic Plants*, Y. P. S. Bajaj, ed., Vol. 11, Springer-Verlag, Berlin, pp. 157-176, (1998).
Strobel, J., M. Hieke, and D. Groger, ''Increased Anthraquinone Production in Galium Vernum Cell Cultures Induced by Polymeric Adsorbents,'' *Plant Cell Tiss. Org. Cult.*, **24**, 207 (1991).
Taticek, R. A., C. W. Lee, and M. L. Shuler, ''Large Scale Insect and Plant Cell Culture,'' *Curr. Opin. Biotechnol.*, **5**, 165 (1994).
Verlaan, P., J. Tramper, K. Ventriet, and K. C. A. M. Luyben, ''A Hydrodynamic Model for an Airlift-Loop Bioreactor with External Loop,'' *Chem. Eng. J. Biochem. Eng. J.*, **33**, B43 (1986).
Verlaan, P., A. M. M. Vaneijs, J. Tramper, K. Vantriet, and K. C. A. M. Luyben, ''Estimation of Axial Dispersion in Individual Sections of an Airlift-Loop Reactor,'' *Chem. Eng. Sci.*, **44**, 1139 (1989).
Vunjak-Novakovic, G., L. E. Freed, J. R. Biron, and R. Langer, ''Effects of Mixing on the Composition and Morphology of Tissue-Engineered Cartilage,'' *AIChE J.*, **42**(3), 850 (1996).
Wilke, C. R., and P. Chang, ''Correlation of Diffusion Coefficients in Dilute Solutions,'' *AIChE J.*, **1**, 264 (1955).

Manuscript received Aug. 12, 1998, and revision received Jan. 10, 2000.